A Low-Cost Titanium Suboxide pH Sensor with Competitive Operational Lifetime Assessed with Electrochemical Impedance Spectroscopy

Kyriakos Almpanidis[a], Apostolos Panagiotopoulos[a], George Kakavelakis[b], Leslie Askew[a], Xiaoqian Pu[a], Dimitar I. Kutsarov[a], Steven J. Hinder[c], S. Ravi P. Silva[a,d] and Vlad Stolojan[a,d,*]

[a] Advanced Technology Institute, School of Computer Science and Electronic Engineering, University of Surrey, Guildford, UK, GU2 7XH

[b] Department of Electronic Engineering, School of Engineering, Hellenic Mediterranean University, Romanou 3, Chalepa, Chania, Crete, Greece, 731 33

[c] Surface Analysis Laboratory, School of Mechanical Engineering Sciences, University of Surrey, Guildford, UK, GU2 7XH

[d] Institute for Sustainability, University of Surrey, Guildford, UK, GU2 7XH

[*] Corresponding author: v.stolojan@surrey.ac.uk

Keywords: pH sensors, Electrochemical Impedance Spectroscopy, Smart Bandages, Wound Monitoring, Transition Metal Oxides

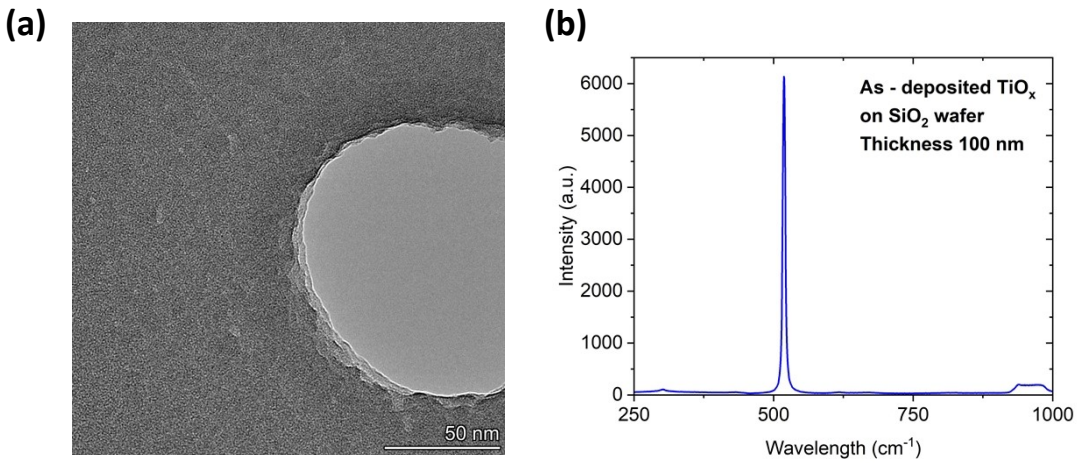

Figure S1. (a) TEM image of the amorphous TiOx film. The hole on the right is due to the TEM grid for resolution purposes. (b) Raman Spectra of a 100 nm TiOx film on a Silicon/silicon dioxide wafer. Since the TiOx films are amorphous, the only peaks that can be observed are those from the Silicon/silicon dioxide wafer.

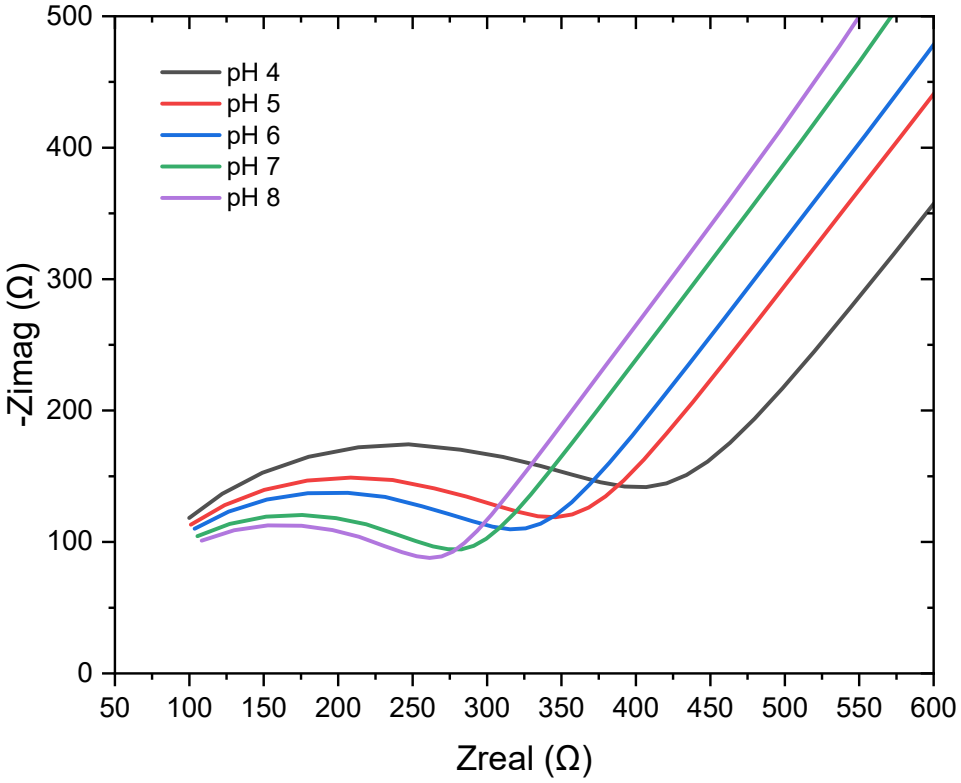

Figure S2. Nyquist plots from the TiO_x sensor in the pH range 4-8. The semicircle evolution is related to interfacial capacitive phenomena.

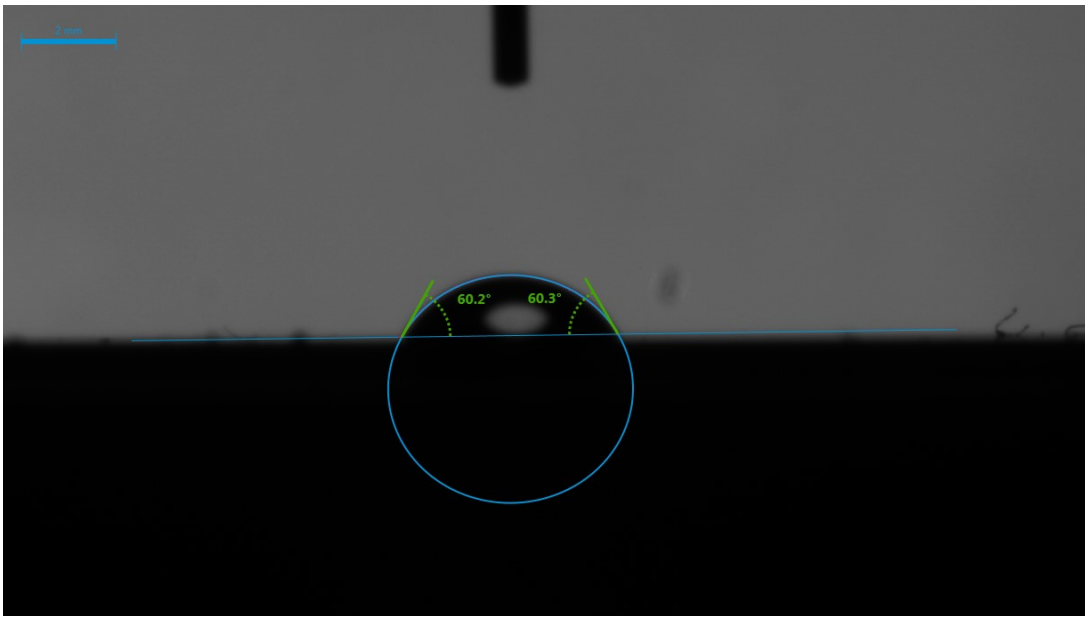

Figure S3. Contact angle measurement for the TiO_x films. The Contact angle of 60.2 degrees indicates the hydrophilicity of the TiO_x film, which can be correlated with the presence of- OH groups on the surface, which are correlated with the TiO_x pH sensing mechanism.

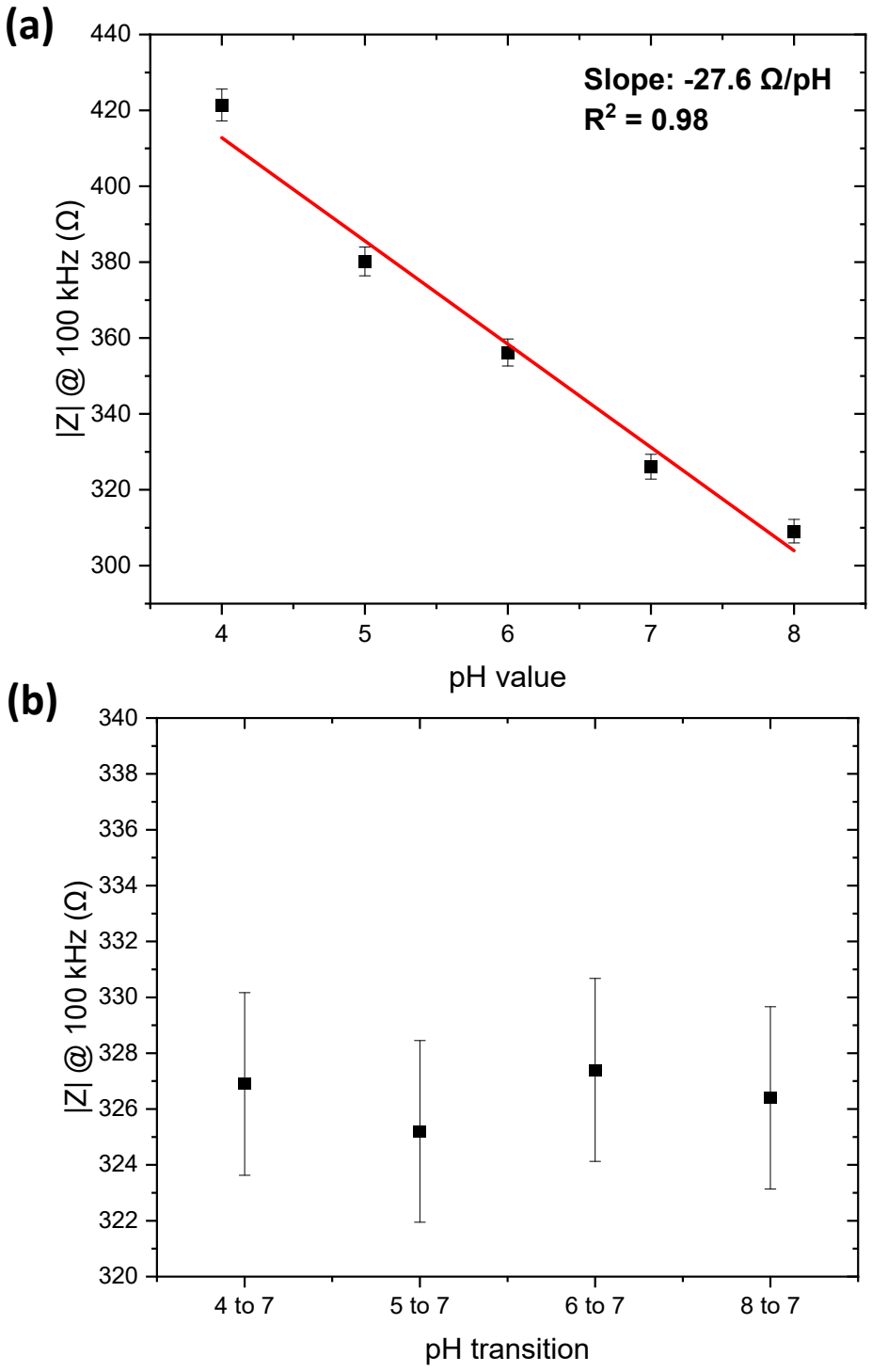

Figure S4. The reversibility of the TiO_x sensor by measuring the impedance at pH 7 after every pH value. (a) The sensitivity in the pH range 4-8 remains constant. (b) pH 7 impedance measured after every pH value. It remained constant which proofs the TiO_x's sensor reversibility. Each error bar is produced by EIS measurements of seven devices.

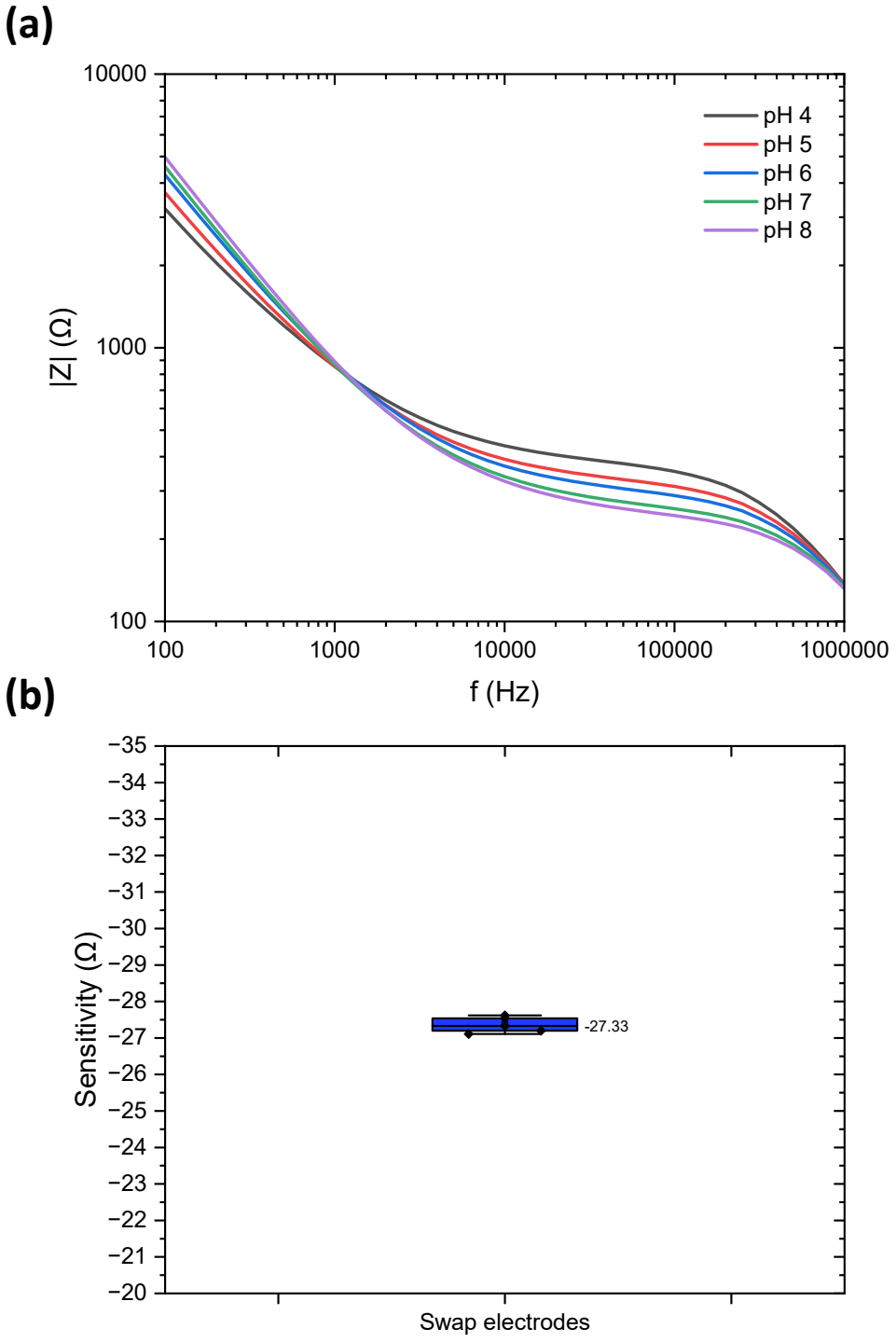

Figure S5. The EIS results for the TiO_x sensors after swapping electrodes. (a) Bode plots responses from the pH4-8 buffer solutions and (b) the sensitivity of the TiOx sensors. The sensitivity maintenance is translated as the sensing mechanism happens on the TiO_x surface.

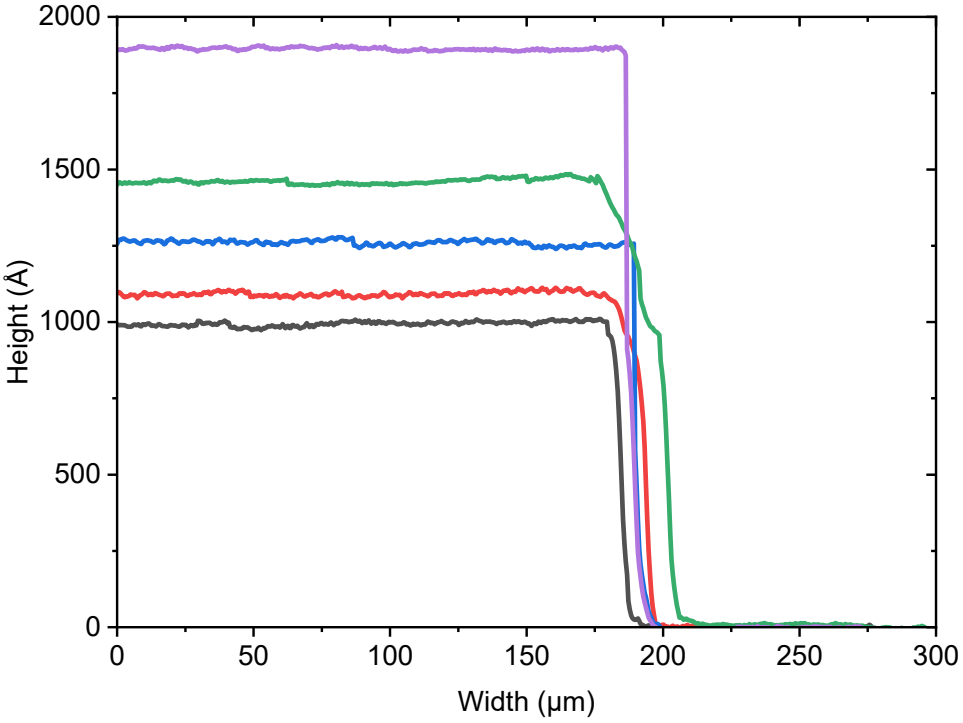

Figure S6. The thicknesses for the Ag electrode (grey line) and the TiO_x films on top of the Ag electrode. The TiO_x thicknesses are 10, 25, 45 and 90 nm, respectively.

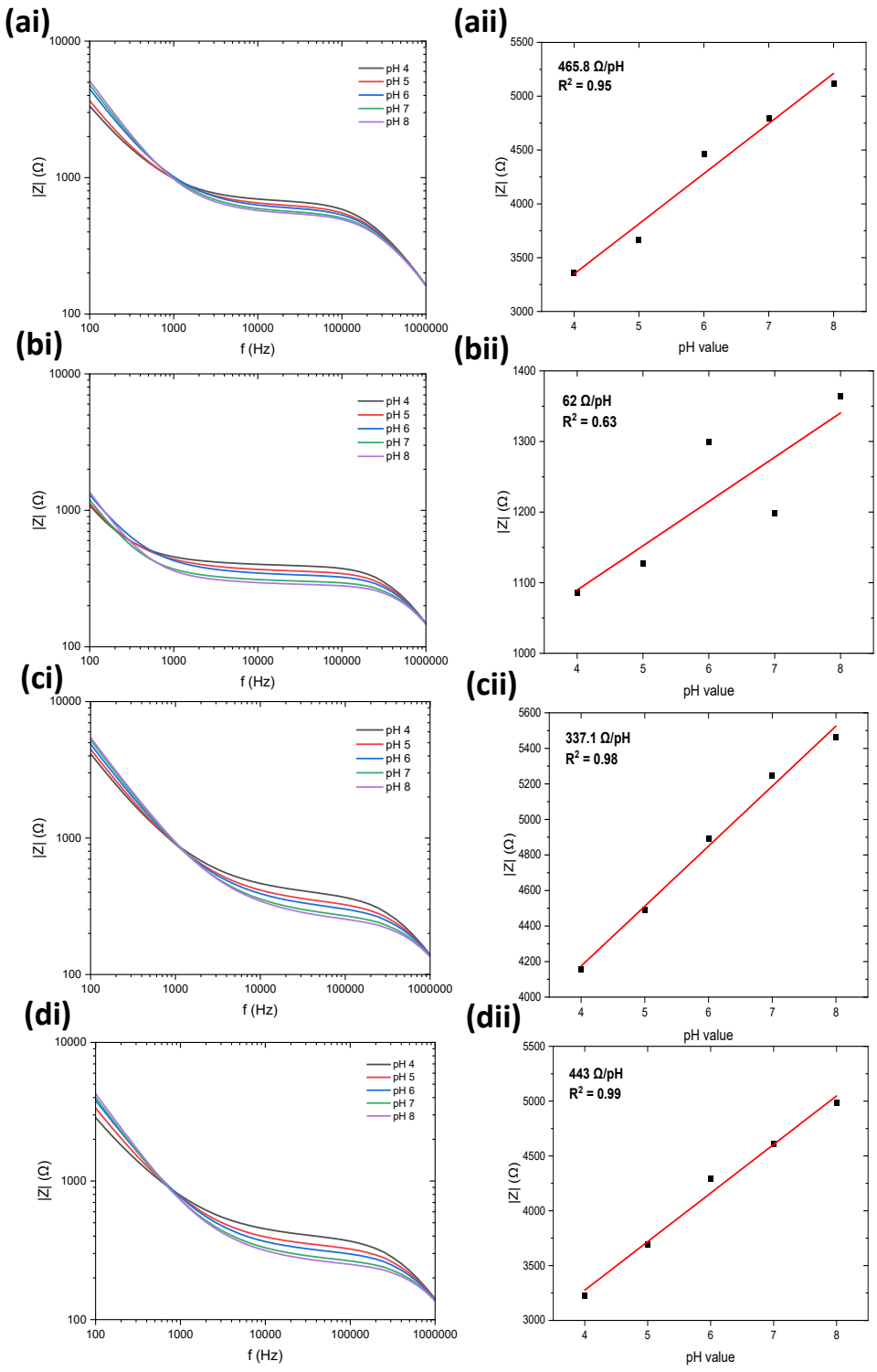

Figure S7. The impedance response for the different TiO_x thicknesses. (ai-di) Bode plots and (aii-dii) Impedance at 100 Hz for every pH in the range 4-8. There is no constant slope (sensitivity) across different TiO_x thicknesses. The a, b, c and d notify the 10, 25, 40 and 90 nm TiOx thickness respectively.

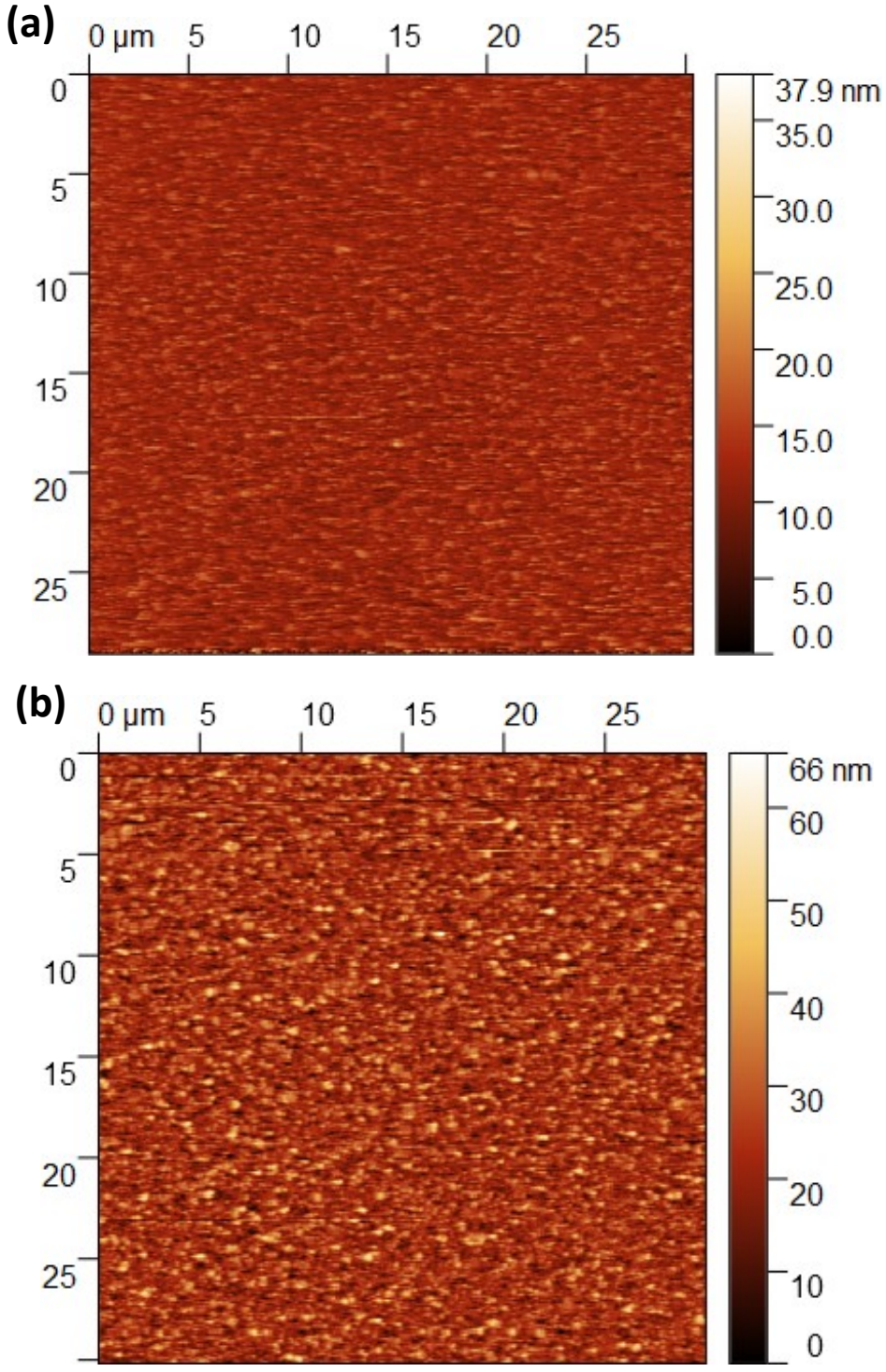

Figure S8. AFM measurements for the Ag electrode. (a) Pristine Ag electrode, (b) after thermal annealing. The roughness increased but there is no islands' formation.

Statistical Significance Analysis

First, the statistical data from pH EIS values at 100 kHz (Figures 3b and d) have been presented below.

TiO_x

pH transition	h-value	p-value
4 to 5	1	$2.14 * 10^{-13}$
5 to 6	1	$6.20 * 10^{-10}$
6 to 7	1	$1.62 * 10^{-13}$
7 to 8	1	$1.89 * 10^{-8}$

PANI

pH transition	h-value	p-value
4 to 5	1	$3.51 * 10^{-9}$
5 to 6	1	$1.05 * 10^{-7}$
6 to 7	1	$1.59 * 10^{-11}$
7 to 8	1	$3.22 * 10^{-11}$

Testing pH sensors with different TiO_x thicknesses, from pH 4 to 8 (Figure 5a)

Comparison	h-value	p-value
Thickness 10 nm with 25 nm	0	0.23
Thickness 10 nm with 40 nm	0	0.127
Thickness 10 nm with 90 nm	0	0.77

Testing pH sensors with different TiO_x thicknesses, from pH 8 to 4 (Figure 5b)

Comparison	h-value	p-value
Thickness 10 nm with 25 nm	0	0.07
Thickness 10 nm with 40 nm	0	0.20
Thickness 10 nm with 90 nm	0	0.16

Comparison	Figure	Material	h-value	p-value
Dilution – Before/After	6a	TiO_x	0	0.3906
Annealing – Fresh/After	6b	TiO_x	1	$1.22 * 10^{-4}$
Stability – pH 4 (Day 1 vs 31)	7a	TiO_x	1	$8.01 * 10^{-9}$
Stability – pH 4 (Day 1 vs 31)	7a	PANI	1	$9.19 * 10^{-11}$
Stability – pH 8 (Day 1 vs 31)	7b	TiO_x	1	$1.28 * 10^{-8}$
Stability – pH 8 (Day 1 vs 31)	7b	PANI	1	$8.47 * 10^{-7}$
Stability – Sensitivity (Day 1 vs 31)	7c	TiO_x	1	$4.17 * 10^{-4}$
Stability – Sensitivity (Day 1 vs 31)	7c	PANI	1	$2.53 * 10^{-4}$

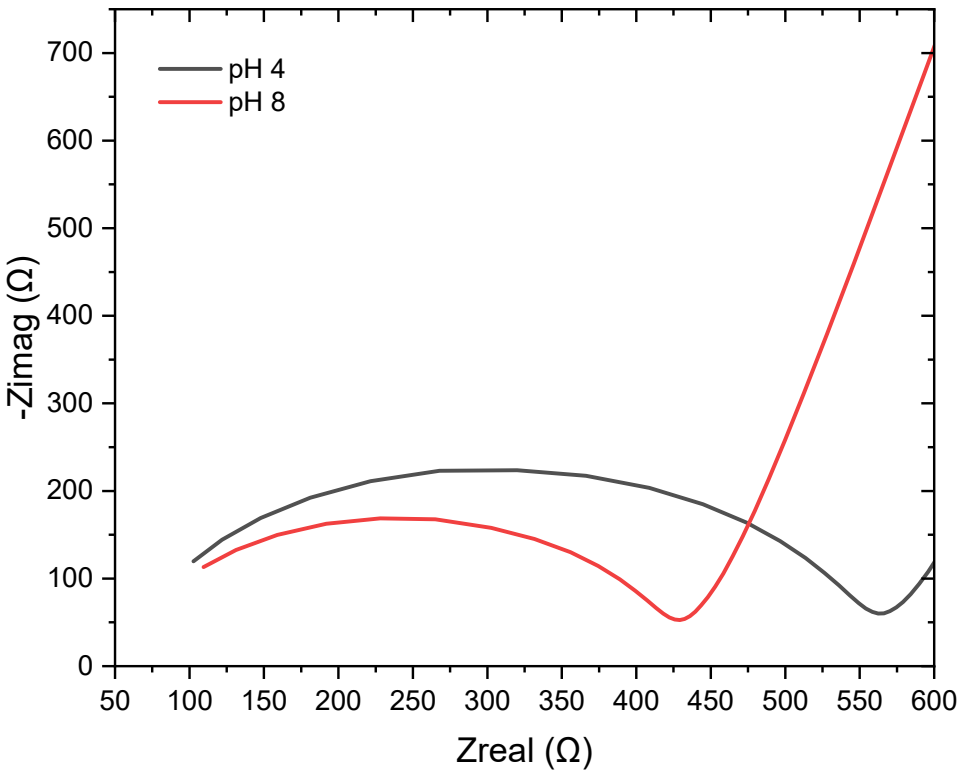

Figure S9. Nyquist plots from the diluted McIlvaine buffer solutions for pH 4 and pH 8. The real axis shift remains the same as the one can be observed from the pristine buffer solution ones (see Figure 9 and S1). This means that the real axis shift can be correlated with the Ag series resistance.

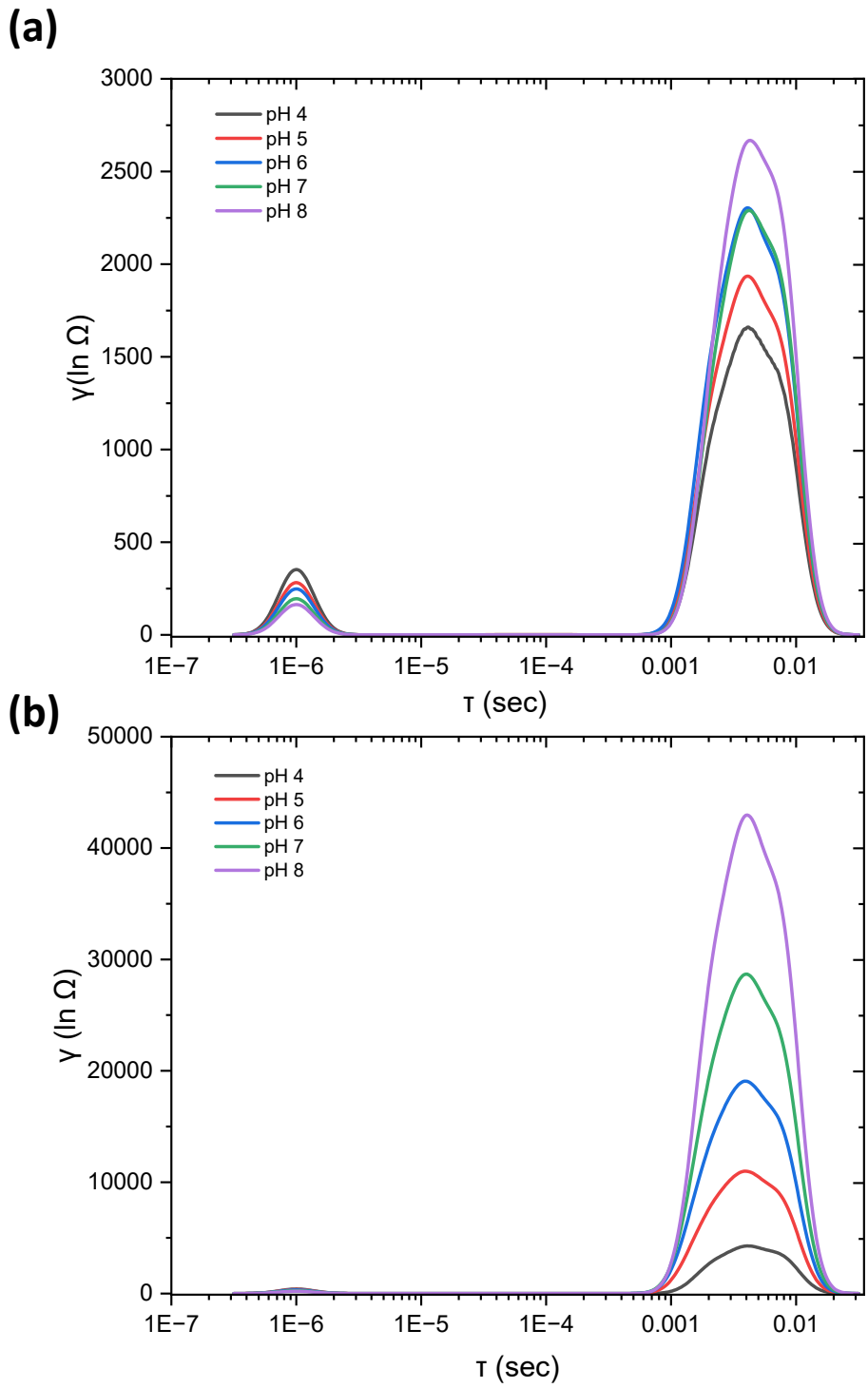

Figure S10. The full spectrum of the DRT data for (a) the TiO_x films and (b) the PANI films. In both spectra there are two processes: one fast (around 10-6 sec, resistive-capacitive phenomena) and one slow (0.005 sec, ionic phenomena).

Equivalent Circuit Analysis

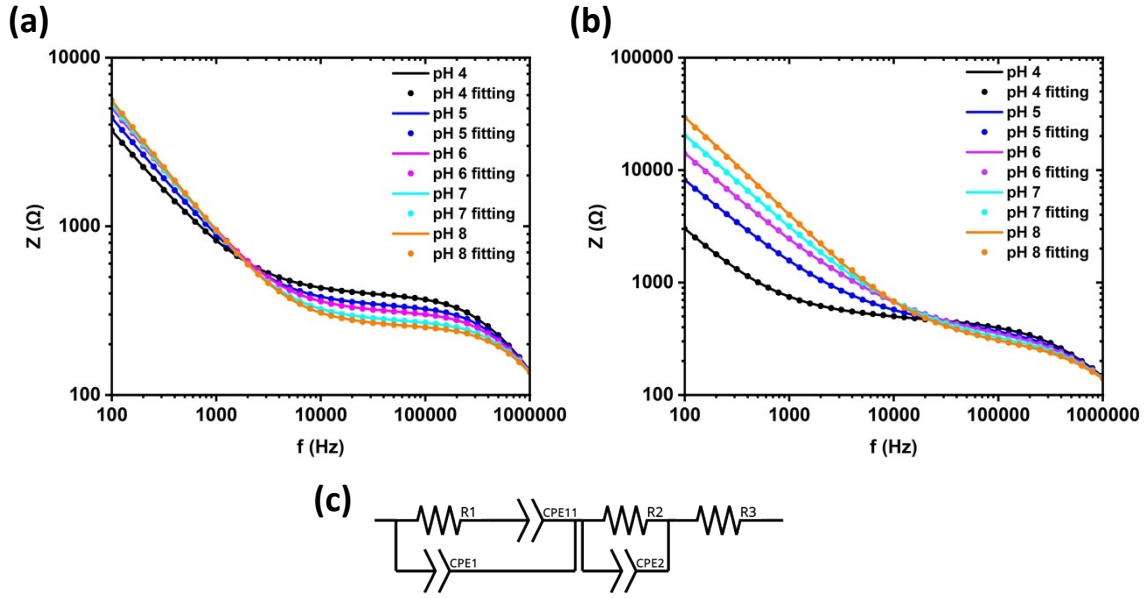

Figure S11. The Bode plots (raw data and equivalent circuit fitting) for (a) TiO_x and (b) PANI pH sensors, respectively. (c) The equivalent circuit used for the EIS fitting. Two time constants have been derived and can be related to the diffusion and interfacial properties of the TiOx and PANI films, as the DRT analysis shows.

TiO_x pH sensor

pH	R_1 (Ω)	R_2 (Ω)	R_3 (Ω)	CPE_1 (Mag) (nF)	CPE_1 (n)
4	350.9	1379	32.59	2.8	0.9448
5	301.1	933.7	33.64	2.57	0.949
6	275.7	520.7	34.3	2.5	0.9506
7	239.1	150.8	35.2	2.28	0.9562
8	217.6	83.05	36.8	1.89	0.965

CPE_{11} (Mag) (nF)	CPE_{11} (n)	CPE_2 (Mag) (nF)	CPE_2 (n)
1200	0.8711	14000	0.658
1100	0.848	6260	0.7569
1010	0.8312	4280	0.846
929	0.829	2110	0.997
851	0.8325	3040	1

PANI pH sensor

pH	R_1 (Ω)	R_2 (Ω)	R_3 (Ω)	CPE_1 (Mag) (nF)	CPE_1 (n)
4	301.1	187.8	42.22	3.46	0.947
5	220.4	232.2	47.74	2.6	1
6	245.5	247.7	52.35	2.29	0.973
7	225.7	114.5	57.02	1.89	0.984
8	212.9	101.1	59.07	1.58	1

CPE_{11} (Mag) (nF)	CPE_{11} (n)	CPE_2 (Mag) (nF)	CPE_2 (n)
1590	0.839	5510	0.562

848	0.775	4160	0.565
449	0.787	3180	0.638
257	0.815	2320	0.69
125	0.86	1500	0.72

The transfer function (Laplace domain) of the equivalent impedance can be approximated by the equation below:

$$Z(s) = \frac{as^3 + bs^2 + cs + d}{s(R_1C_1C_{11}s + C_1 + C_{11})(R_2C_2s + 1)}$$

with

$a = R_1R_2C_{11}R_3C_2$

$b = R_1C_{11}R_2(C_1 + C_{11}) + R_3(R_1C_{11} + R_2C_2(C_1 + C_{11}))$

$c = R_1C_{11} + R_2C_2(R_1 + R_3)(C_1 + C_{11})$

$d = 1$

Hence, this transfer function has one differentiator and two poles (t_1 and t_2). The extracted numerical values of the time constants can be found in the tables below:

pH value	**t_1 (sec)**	**t_2 (sec)**	**t_1 (sec)**	**t_2 (sec)**
	TiO_x		**PANI**	
4	$9.83 * 10^{-7}$	$1.93 * 10^{-2}$	$1.04 * 10^{-6}$	$1.04 * 10^{-3}$
5	$7.75 * 10^{-7}$	$5.84 * 10^{-3}$	$5.73 * 10^{-7}$	$9.66 * 10^{-4}$
6	$6.89 * 10^{-7}$	$2.23 * 10^{-3}$	$5.63 * 10^{-7}$	$7.88 * 10^{-4}$
7	$5.45 * 10^{-7}$	$3.18 * 10^{-4}$	$4.25 * 10^{-7}$	$2.65 * 10^{-4}$
8	$4.11 * 10^{-7}$	$2.53 * 10^{-4}$	$3.36 * 10^{-7}$	$1.52 * 10^{-4}$

Regarding the stability study, the equivalent circuits for the degraded devices can be found below:

TiO_x pH sensor

pH – Day	**R_1 (Ω)**	**R_2 (Ω)**	**R_3 (Ω)**	**CPE_1 (Mag) (nF)**	**CPE_1 (n)**
pH 4 – Day 17	356.2	101	62.7	1.55	0.988
pH 4 – Day 31	362.9	99.63	58.3	1.46	0.992
pH 8 – Day 17	225.2	1050	61.01	2.11	0.965
pH 8 – Day 31	232.2	1042	69.01	2.05	0.969

CPE_{11} (Mag) (nF)	**CPE_{11} (n)**	**CPE_2 (Mag) (nF)**	**CPE_2 (n)**
2613	0.834	20220	0.834
2643	0.79	21500	0.55
960	0.78	15210	0.94
972	0.771	15910	0.934

PANI pH sensor

pH – Day	R_1 (Ω)	R_2 (Ω)	R_3 (Ω)	CPE_1 (Mag) (nF)	CPE_1 (n)
pH 4 – Day 10	328	123.5	62.6	1.653	0.986
pH 4 – Day 31	327	122	63.5	1.64	0.984
pH 8 – Day 10	210.1	281.2	58.17	2.273	0.971
pH 8 – Day 31	208.2	280.4	59.3	2.24	0.968

CPE_{11} (Mag) (nF)	CPE_{11} (n)	CPE_2 (Mag) (nF)	CPE_2 (n)
244	0.76	4001	1
248	0.763	4055	1
237	0.822	2700	0.86
239	0.827	2720	0.863

The extracted numerical values of the time constants can be found in the tables below:

pH – Day	t_1 (sec)	t_2 (sec)	pH – Day	t_1 (sec)	t_2 (sec)
	TiO_x			**PANI**	
pH 4 – Day 17	$5.52 * 10^{-7}$	$2 * 10^{-3}$	**pH 4 – Day 10**	$5.42 * 10^{-7}$	$4.9 * 10^{-4}$
pH 4 – Day 31	$5.29 * 10^{-7}$	$2.1 * 10^{-3}$	**pH 4 – Day 31**	$5.36 * 10^{-7}$	$4.91 * 10^{-4}$
pH 8 – Day 17	$4.75 * 10^{-7}$	$1.5 * 10^{-2}$	**pH 8 – Day 10**	$4.77 * 10^{-7}$	$7.5 * 10^{-4}$
pH 8 – Day 31	$4.76 * 10^{-7}$	$1.6 * 10^{-2}$	**pH 8 – Day 31**	$4.66 * 10^{-7}$	$7.6 * 10^{-4}$

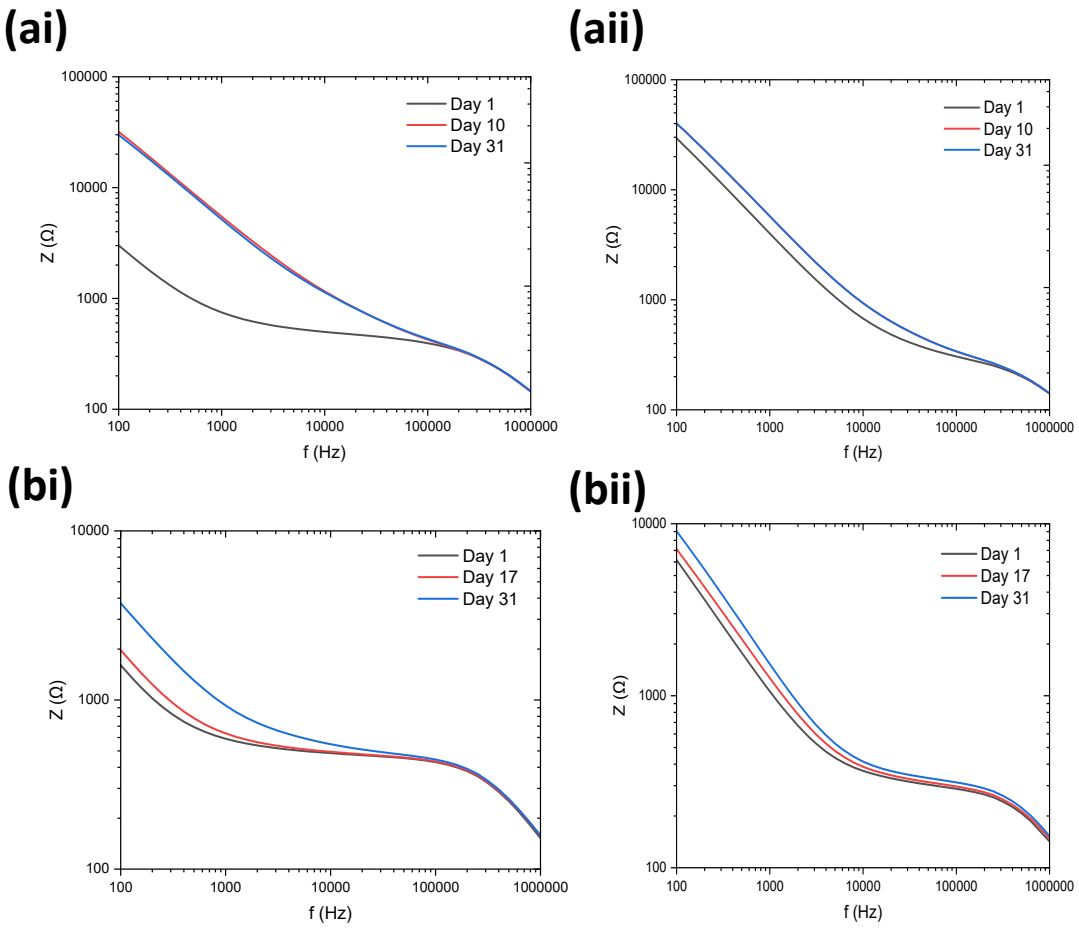

Figure S12. Bode plots for the one-month time stability experiments, for TiO_x (ai - aii) and PANI (bi - bii). The i and ii notify the pH 4 and pH 8 study, respectively. From the shift at low-frequencies, it can be derived that the diffusion-related phenomena are mostly affected after the 31-day stability experiments.

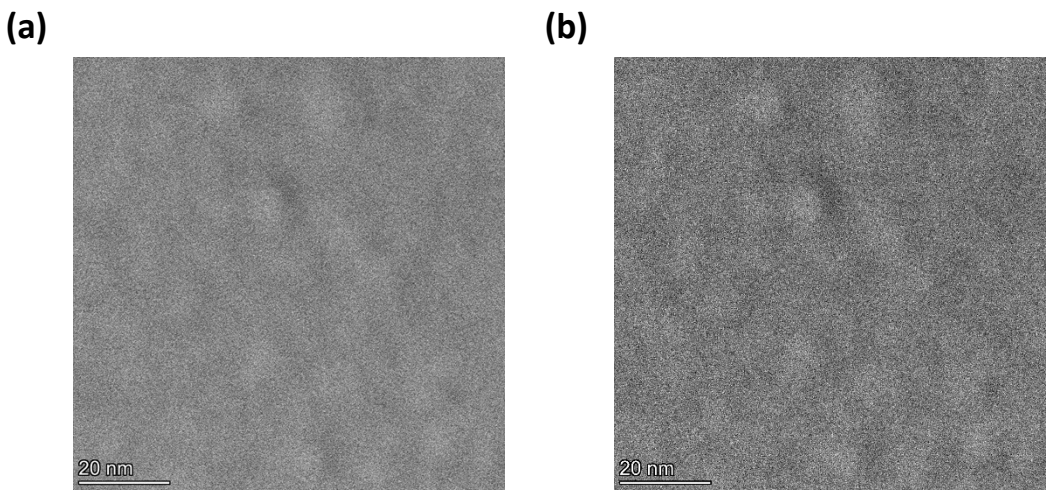

Figure S13. (a) HAADF-STEM image of the TiO_x film, (b) DF-STEM image of the TiO_x film. The contrast is related to the namometre level non-uniformities of the film surface.

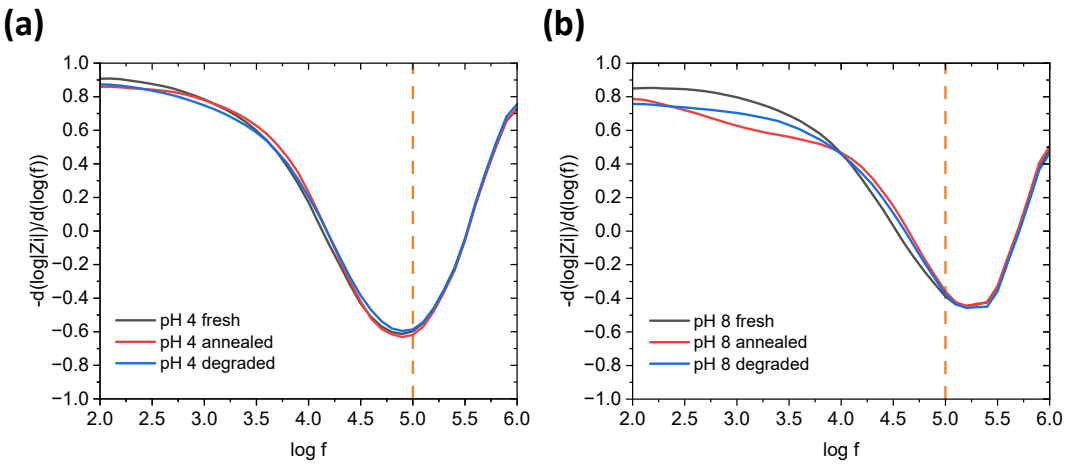

Figure S14. The effective CPE-like phase parameter α over frequency for (a) pH 4, (b) pH 8, respectively. The frequency of 100 kHz is denoted with the orange dashed line. The changes in the frequency's position, the magnitude of the global minimum and the depth are minimal. Also, the frequency of 100 kHz lies near the global minimum of the spectra, so the slope-based sensitivity is reduced. Hence, at the frequency of 100 kHz, any porosity and/or adsorbed water produce smaller EIS signal variations relative to regions with steeper slopes.

Table S1. A comparison table for the stability of various pH electrochemical biosensors.

Reference	Sensing material(s)	Electrode material	Method	Sensitivity	Stability & Protocol
[23]	PANI-IrO_2/Nafion	Au	OCP	-69.1 mV/pH	14 days (~1% loss, at pH 7.3 only)
[26]	IrO_2	Pt	OCP	-77 mV/pH	6 weeks (x8 higher response time, x2 higher at 4 weeks)
[27]	IrO_2	Au	OCP	-74 mV/pH	7 days stability at pH 4, 7 and 9.
[36]	IrO_2	Au	OCP	-69.43 mV/pH	ΔE=0.76 mV/pH after 15 hours, at pH 8.
[37]	PANI/IrO_x	Au	OCP	-59.1 mV/pH	3.5 mV drift after 30 days (stability in PBS only)
[38]	PANI	Ag/AgCl	OCP	-62.4 mV/pH	3 mV/hour for 14 hours (~15% loss)
[39]	TiO_2	-	OCP	1.16 dBm/pH	25% loss after 4 days.
[40]	Al_2O_3	Si	C-V measurements (flat-band potential)	-56 mV/pH	0.35 mV/day drift, 600 days (pH 7 only, substrate heating at 800°C) Sensitivity almost same.
[41]	IrO_2	Pt	OCP	-69.89 mV/pH	1 year (sensitivity loss 20% after 30 days)
This work	**TiO_x**	**Ag**	**EIS**	**-27.8 Ω/pH**	**Stability 31 days. 5.65% increase at pH 4, 3.8% increase at pH 8, 2.25% sensitivity loss.**